

Analysis of Various Yaw Control Techniques for Large Wind Turbines

Wael Farag*, Manal El-Hosary, Ahmed Kamel and Khaled El-Metwally

*College of Eng. & Tech., American University of the Middle East, Kuwait

Electrical Power Dept., Cairo University, Egypt

*Corresponding Author: wael.farag@aum.edu.kw, wael.farag@cu.edu.eg

ABSTRACT

In this paper, we introduce three different nacelle yaw controllers that use distinct techniques and study their performances in improving the captured energy by the turbine. The first one is a carefully tuned Proportional-Integral-Differential (PID) controller with its simple design; the second one is a linguistic fuzzy logic controller with its intuitive flexible design; and the third one is a Model-Predictive-Controller (MPC) with its adaptive functionality. The control objective of the developed controllers is to effectively track the wind direction by the yaw motion of the turbine nacelle, and consequently to improve the energy capture. A comparative study and a thorough analysis of the performances of three controllers are carried out using extensive MATLAB/SIMULINK simulations.

Keywords: Wind Turbine, Yaw Control, Yaw Error, PID, Fuzzy Logic Controller, Model Predictive Control (MPC).

1. INTRODUCTION

To reduce the cost of energy produced by wind turbines and to make them competitive to conventional power plants, these can be considered as the main goal of wind turbine optimization and the wind energy generation industry (Kim *et al.*, 2014). Therefore, the current trend of this industry is to use large and ultra-large wind turbines that reach more than 10 MW in rating, especially in off-shore wind farms, as such turbines proved to be more efficient.

A typical wind turbine consists of three main components: (1) the nacelle, which contains the key components of the wind turbine, including the gearbox and the electrical generator; (2) the tower, which carries the nacelle; and (3) the rotor and its blades, which capture the wind energy and transfer its power to the rotor hub and then to the electrical generator.

In the last two decades, many types of research had discussed how to maximize wind energy extracted from wind turbines (Farag *et al.*, 2016; Hassan *et al.*, 2011, 2012). The local control systems in wind turbines are responsible for controlling each element of wind turbine individually such as pitch control system (Hassan *et al.*, 2011, 2012), yaw control (Kim *et al.*, 2014; Farag *et al.*, 2016; Farag *et al.*, 2017), and generator torque control (Hemeida *et al.*, 2011, 2013; Shariatpanah *et al.*, 2013).

Pitch control and generator torque control have the biggest share in researchers' interest (Hassan *et al.*, 2011, 2012; Farag *et al.*, 2017; Hemeida *et al.*, 2011, 2013; Shariatpanah *et al.*, 2013) as they have a noticeable effect on energy harvest; on the other hand, nacelle yaw control has lower interest among researchers due to its unnoticeable effect on small and medium size turbines (few hundreds KWs) (Shariatpanah *et al.*, 2013). However, since the industry trend is to use multi-mega-watts wind turbine capacities, sophisticated nacelle control becomes necessary for both power extraction and the protection of the internal components (Kim *et al.*, 2014).

As an example of previous work in yaw control, Wenzhou *et al.* (2011) use self-adaptive Fuzzy PID based servo controller to control the yaw system by generating K_p , K_i and K_d from the Fuzzy logic based controller, which takes

the yaw-angle error as input and calculates the yaw actuator torque required to minimize this error for best wind tracking. However, the authors tested their controller by only using a step input to represent a wind direction change and they reported that the nacelle followed successfully the variations in the input signal. Actually, this work is not showing that the inertia and the time constant of the nacelle are being taken into consideration. Additionally, it does not show enough results to prove the effectiveness of the proposed control technique given its complexity against more conventional techniques. Another example is the work of Shariatpanah *et al.* (2013) where two PI controllers that work in different regions are proposed mainly to protect the WT against over speed and excess power not to maximize the captured power. Moreover, by developing a sensorless yaw control, Farret *et al.* (2001) have estimated the maximum wind power that corresponds to the optimum wind direction. A fuzzy PID system for yaw position control is designed by Chen *et al.* (2009) to track precisely the wind direction. A fixed-speed wind turbine has been simulated by Fadaeinedjad *et al.* (2009) with all aerodynamic, mechanical, and electrical aspects taken into consideration. He also estimated the yaw errors that lead to the voltage and power oscillations. The power output of a given wind turbine has been significantly enhanced by Kusiak *et al.* (2010) by optimizing the yaw angle of the blade by using an evolutionary computational algorithm. An accurate yawing torque has been obtained using a maximum power point tracking algorithm that has been implemented by Lee *et al.* (2011). The recorded wind direction signals have been processed through an electronic yaw controller by Rijanto *et al.* (2011) and were successfully able to dissipate the cyclic instabilities of a horizontal-axis wind turbine. As an interesting endeavor, an intelligent yaw controller based on the artificial neuro-endocrine-immunity system is proposed by Chenghui *et al.* (2011), which significantly improved the stability and robustness of the yaw control system. In addition to that, yaw position forecasting becomes a subject of several interesting academic studies (Yesilbudak *et al.*, 2015). Instead of using direct control of individual turbines, a collective yaw control is proposed (Yesilbudak *et al.*, 2015).

2. NACELLE YAW SYSTEM

Yaw denotes the rotation of the nacelle and the rotor about the vertical tower axis. The yaw system provides a mechanism to yaw the nacelle and to keep the rotor axis aligned with the direction of the wind in order to obtain maximum power extraction from wind (Kim *et al.*, 2014). The yaw system is located between the wind turbine nacelle and tower as shown in Fig. 1. The wind turbine is said to have a yaw error if the rotor is not perpendicular to the wind.

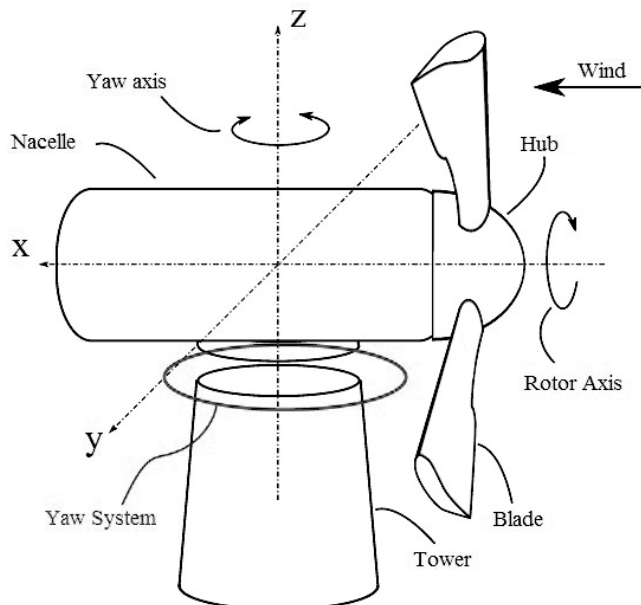


Fig. 1. Nacelle yaw system.

3. YAW ERROR EFFECT ON HARVESTED POWER

If the rotor acting as a solid disk and wind components parallel to the rotor plane did not have any effect on the rotor, the difference in power would be a factor of $\cos^3(\psi)$ (Santoso *et al.*, 2011), where ψ is the yaw error angle.

This \cos^3 factor is derived from the fact that the component of the wind velocity normal to the rotor plane has a magnitude that is scaled by the cosine of the yaw error angle from the magnitude of the wind speed and the cube is a result of the fact that the power in the wind is a function of the cube of the wind speed (Santoso *et al.*, 2011).

In our current work, we verify this loss factor by adding the “Power” equation (1) to the wind turbine model in Farret *et al.* (2001) in order to illustrate the yaw error effect on the harvested power.

$$P_w = \frac{1}{2} \pi \rho C_p(\beta, \lambda) R^2 (V_w \cos \psi)^3 \dots\dots\dots (1)$$

where P_w is the turbine harvested power in *Watts*, ρ is the density of air in Kg/m^3 , C_p is the rotor power coefficient with is a function of β (the pitch angle in $^\circ$) and λ (the blade tip-speed ratio), R is the rotor radius (~ blade length) in *meters*, V_m is the wind velocity in *meter/sec.* and ψ is the yaw error angle.

Using different wind profiles where the wind speed is maintained constant at 10 m/s and the wind directions are varying at angles of 0° (means no yaw error), 5° (yaw error = 5°), 10° (yaw error = 10°), 20° (yaw error = 20°), and 30° (yaw error = 30°), these values are chosen based on the turbine specification of the maximum allowable yaw angle, considering nacelle mechanical limitations, of $\pm 30^\circ$ with yaw rate $0.5^\circ \sim 1^\circ$ per second.

As shown in Fig. 2, the results indicate that the power is at its maximum value when nacelle is aligned with wind direction (zero yaw error) and it decreases dramatically with the increase of the yaw error as it reaches only 65% @ 30° . Fig. 2 also proves that the output of the model matches the $\cos^3(\psi)$ equation.

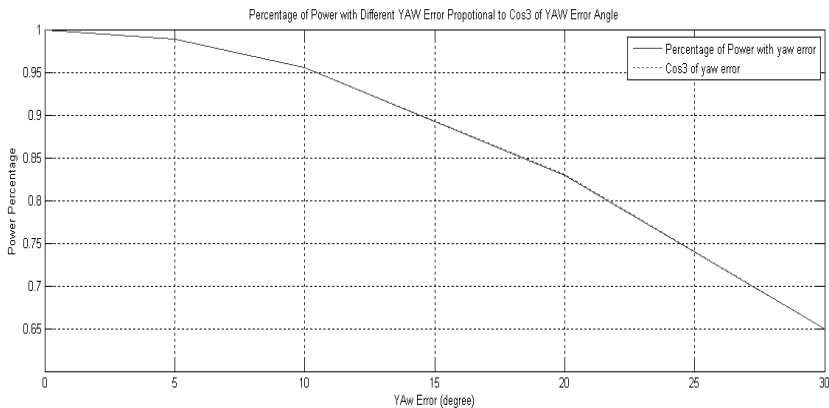


Fig. 2. The \cos^3 factor of wind turbine power and yaw error.

4. MODELLING AND CONTROL

For a system as complex as a wind turbine, the ability to simulate the physical systems (mechanical, electrical, hydraulic, etc.) and control systems in a single environment is crucial to the development process.

The comprehensive SIMULINK™ model developed in Miller (2013) is used and as shown in Fig. 3 it includes (1) three-dimensional sub-models of the tower, nacelle, and blades that are developed within the SimMechanics™ environment; (2) Hydraulic pitch actuators and electrical yaw actuators models; (3) A simple generator and electrical grid model. The model is fully explained in S. Miller (2009) and can be downloaded from S. Miller (2017) as an open source.

4.1. Wind Turbine Model Overview

The modeled wind turbine is 1.6 MW rating with its topology shown in Fig. 3. In the left side, the physical system is placed, and the supervisory controller at the right side, while the yaw\pitch controller is placed at the center. Moreover, the aerodynamics model, as well as the simulation tools, is placed at the top, while at the bottom, the different signal-scopes are placed.

4.2. Active Yaw Control

Whatever the controller type used in yaw control is, we have the controller reference signal “Wind Direction” measured by the wind direction sensor. The measured feedback signal is nacelle yaw angle. The controller output signal is the torque command to yaw-motor valves (the nacelle is mounted on a roller bearing and the azimuth rotation is achieved via a plurality of powerful hydraulic motors that works the yaw actuator). The valves have mechanical constraints that must be observed in the controller implementation and represented by the Nacelle Yaw Rate (NYR) (Kim *et al.*, 2014). The block diagram of the yaw controller is shown in Fig. 4.

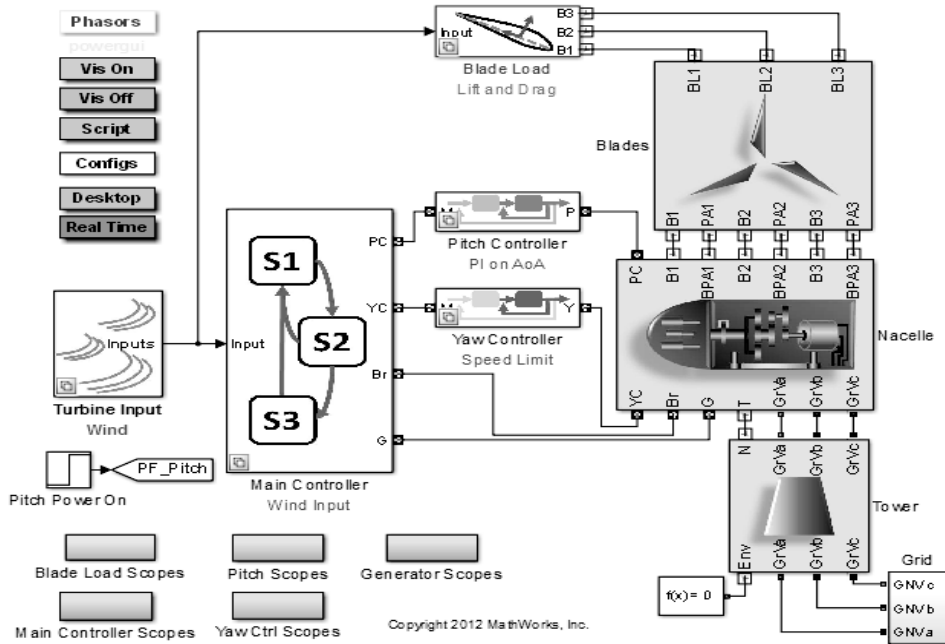


Fig. 3. Wind turbine SIMULINK™ model.

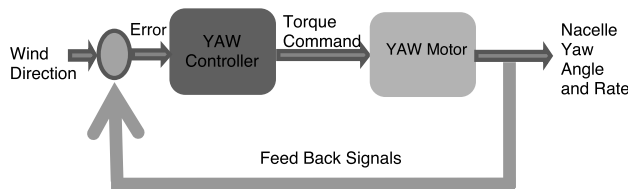


Fig. 4. Active yaw control block diagram.

4.3. Yaw PID Controller

A Proportional–Integral–Derivative controller (PID controller) is a control loop feedback mechanism widely used in industrial control systems and a variety of other applications requiring continuously modulated control. A PID controller continuously calculates an error value $e(t)$ as the difference between the desired Set-Point (SP) and a

measured Process Variable (PV) and applies a correction based on proportional, integral, and derivative terms (denoted K_p , K_i , and K_d , respectively), which give the controller its name.

Tuning a control loop is the adjustment of its control parameters (proportional band/gain, integral gain/reset, derivative gain/rate) to the optimum values for the desired control response. Stability (no unbounded oscillation) is a basic requirement; however, specifically in the yaw-system, it is required to be underdamped producing no oscillation for the hydraulic system.

A PID controller has been developed using SIMULINK to control the nacelle yaw motion. The non-linear wind turbine model described above has been used. Extensive trial and error iterations based on guess-and-check are carried out and using Integral of Time-weighted Absolute Error (ITAE) criterion (Fernando, 2005) as a performance index measure. In this method, the proportional action is the main control, while the integral and derivative actions refine it. The controller gain, K_p , is adjusted with the integral and derivative actions held at a minimum until the desired output (rise time) is obtained, then tuning K_i for a best transient response (overdamped “no overshoot” in our case) while maintaining K_p and K_d at their pre-selected values and next, tuning up K_d for zero steady state error while keeping K_p and K_i at their pre-selected values. The previous steps have been iterated several times till the overall desired system performance is reached.

Three different wind profiles have been used to tune as well as test the PID controller, namely, “Wind Direction 1”, “Wind Direction 2”, and “Wind Direction 3”. The first wind profile “1”, which represents one of the samples used to tune the controller, depicts a profile variable wind directions with abrupt changes (from +ve to -ve) and a constant wind direction segment as well. The other two profiles are mainly used for testing. Profile “2” presents less severe wind direction change than the one the controller was tuned for, and profile “3” presents a more severe case than the one the controller was tuned for.

The top part of Fig. 5 shows the wind profile that is being used to tune up the PID controller at hand. The solid-line shows the desired wind speed and direction, while the dotted-line represents the yaw-system response (angle). It is clear how excellent the yaw angle tracks the wind direction. The gain values used to achieve these results are $K_p = 300$, $K_i = 0.1$, $K_d = 0.0$. The bottom part of Fig. 5 shows the nacelle yaw motion rate (in degrees per second) with the rise time and the overdamped response being illustrated.

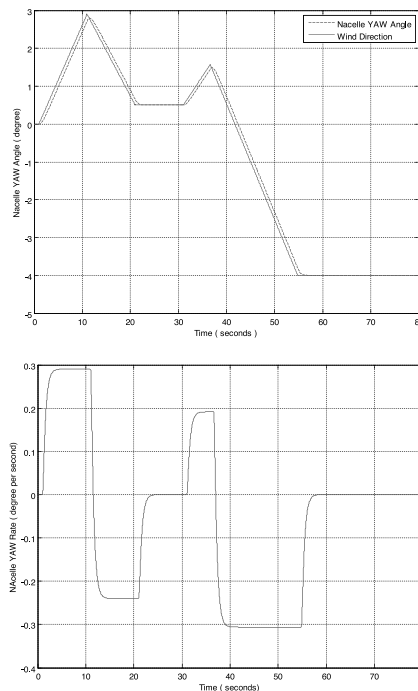


Fig. 5. PID, Top: Nacelle Yaw Angle and “Wind Direction 1”, Bottom: Nacelle Yaw Rate.

It is well known among researchers that PID controllers are not adaptive and once they have been tuned for a certain set of system inputs, they do not necessarily give the same performance using another set or under different system conditions. Consequently, PID controllers must be intensively tested with validation sets of system inputs to confirm performance.

The designed yaw controller has been tested extensively under various wind profiles; two of them are shown in Fig. 6 and 7 denoted as “Wind Direction 2” and “Wind Direction 3”. The excellent performance of the controller is shown in the top parts of the two figures. The bottom parts of the two figures show the nacelle yaw rates.

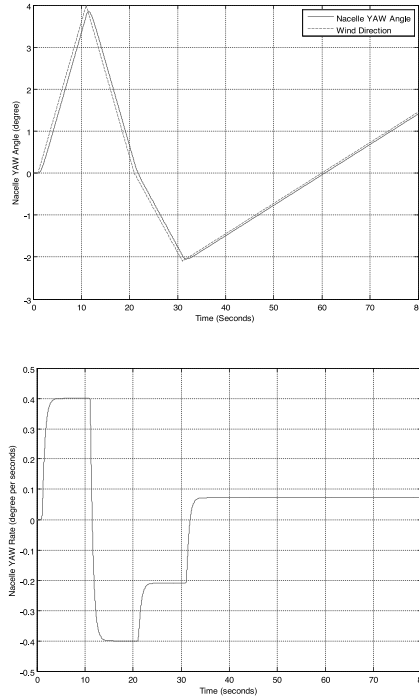


Fig. 6. PID, Top: Nacelle Yaw Angle and “Wind Direction 2”, Bottom: Nacelle Yaw Rate.

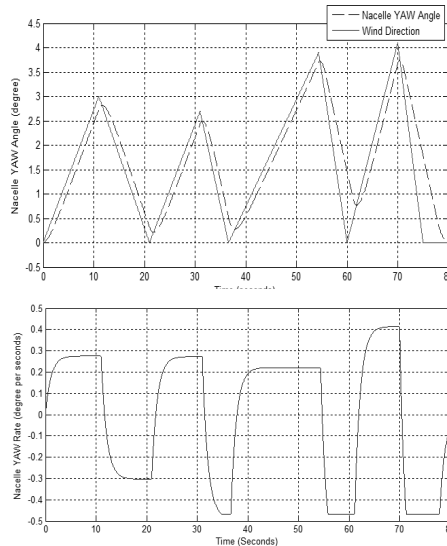


Fig. 7. PID, Top: Nacelle Yaw Angle and “Wind Direction 3”, Bottom: Nacelle YAW Rate.

4.4. Yaw Fuzzy Logic Controller

Fuzzy Logic Controllers (FLC) are very simple conceptually. They consist of an input stage, a processing stage, and an output stage (Fadaeinedjad *et al.*, 2009; Kusiak *et al.*, 2010; Lee *et al.*, 2011). The input stage maps sensor or other inputs to the appropriate membership functions and truth values. The processing stage invokes each appropriate rule and generates a result for each, then combines the results of the rules. Finally, the output stage converts the combined result back into a specific control output value.

The main advantage of FLC is that it does not require precise mathematical models. It is suitable for strong coupling, time-varying and nonlinear system or control as the one we have (Farag *et al.*, 1996).

The yaw FLC structure is chosen to be seven linguistic membership functions for each of its two inputs, “the yaw error” and its “derivative”, and its output, “the torque command to the yaw motor”. The linguistic variables are Negative Big (NB), Negative Medium (NM), Negative Small (NS), Zero (Z), Positive Big (PB), Positive Medium (NM), and Positive Small (PS). This structure results in 49 If-Then rules as shown in Table. 1. The yaw FLC is then normalized using inputs and outputs gains.

The developed FLC code is embedded in a SIMULINK block and inserted in the “yaw controller” of the wind turbine model shown in Fig. 1. The FLC receives two inputs: the yaw error “e” and its derivative “ Δe ” (as they emulate the proportional and the differential term analogous to the PID controller). Membership functions are formed using Gaussian-bell shape functions for the two inputs and singletons for output as shown in Fig. 8. The top part of Fig. 9 shows the wind profile that is being used to tune-up the FLC at hand. The solid-line shows the desired wind speed and direction, while the dotted-line represents the yaw-system response (angle). It is clear how excellent the yaw angle tracks the wind direction. After careful tuning using intuition and extensive trial an error iterations, the normalization gain factors were found to be $K_{error} = 15$, $K_{derror} = 1$, $K_{out} = 430$.

Table 1. Fuzzy Logic Controller IF-Then Rules.

Δe e	NB	NM	NS	Z	PS	PM	PB
NB	-1	-1	-1	-1	-2/3	-1/3	0
NM	-1	-1	-1	-2/3	-1/3	0	1/3
NS	-1	-1	-2/3	-1/3	0	1/3	2/3
Z	-1	-2/3	-1/3	0	1/3	2/3	1
PS	-2/3	-1/3	0	1/3	2/3	1	1
PM	-1/3	0	1/3	2/3	1	1	1
PB	0	1/3	2/3	1	1	1	1

The current FLC is not adaptive as well and the results of its validation using wind profiles as “Wind Direction 2” and “Wind Direction 3” are giving an unsatisfactory performance as shown in Fig. 10 and Fig. 11.

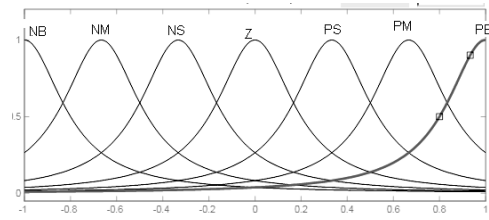


Fig. 8. Gaussian-Bell Shaped Membership Functions for Input Signals.

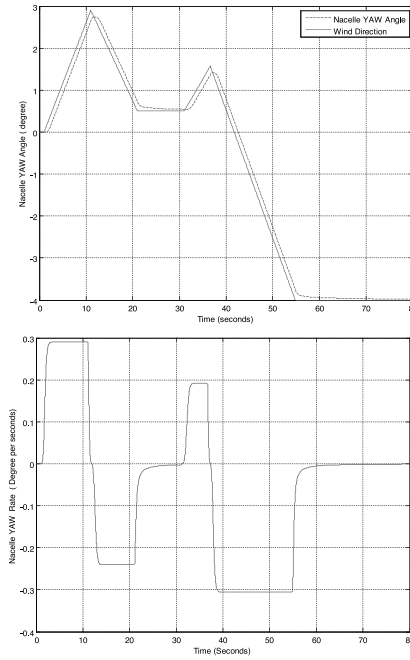


Fig. 9. FLC, Top: Nacelle Yaw Angle and “Wind Direction 1”, Bottom: Nacelle Yaw Rate.

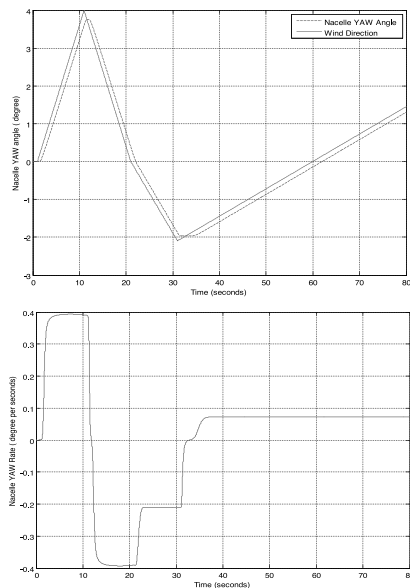


Fig. 10. FLC, Top: Nacelle Yaw Angle and “Wind Direction 2”, Bottom: Nacelle YAW Rate.

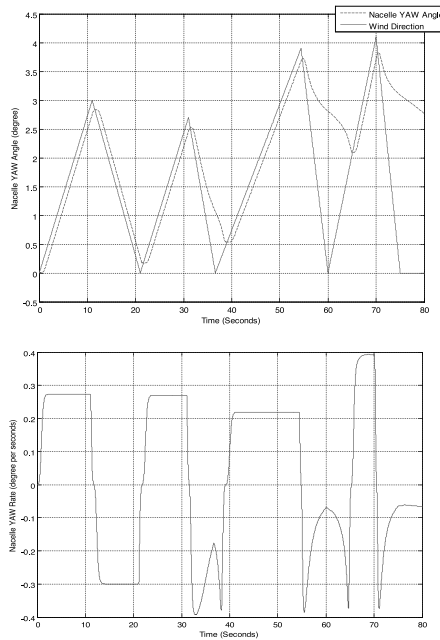


Fig. 11. FLC, Top: Nacelle Yaw Angle and “Wind Direction 3”, Bottom: Nacelle Yaw Rate.

5. YAW MODEL PREDICTIVE CONTROLLER

5.1. MPC Background

The Model Predictive Control, or MPC, is an advanced control technique (Bemporad *et al.*, 2005) that relies on the dynamic model of the plant obtained by system identification and usually used in the form shown in Fig. 12 and Table 2.

Block Diagram of a SISO Model Predictive Control Toolbox Application

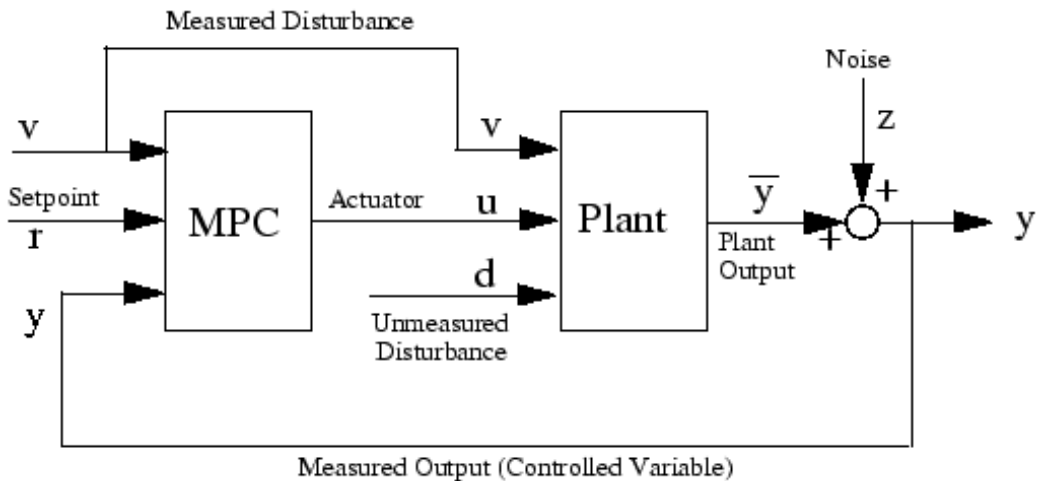


Fig. 12. Model Predictive Control Block Diagram.

Table 2. Model Predictive Control Signals.

r	Set point (or reference). The target value for the output. (Wind Direction Signal)
u	Manipulated variable (or actuator). The signal the controller adjusts in order to achieve its objectives. (Torque Command to Yaw Motor)
v	Measured disturbance (optional). Not used
y	Measured output. Used to estimate the true value (Yaw Angle).
z	Measurement noise. Not used

5.2. Plant Model

The theory of operation of MPC assumes working with linear time-invariant plant models. Because the wind turbine model is a highly non-linear system, then system identification MATLAB toolbox (Wang 2009; Bemporad *et al.*, 2005) is used to get linear time-invariant models of the yaw actuation system. The data is collected from the input (torque command) and the output (yaw angle) measured from the PID-controlled yaw actuator case described in Section 4.3.

Different model structures have been tried by testing their fitness to the collected data (yaw angle measurements). As per the graphs shown in Fig. 13, ARX440 model has been selected as it provides the highest correlation of 85.37%.

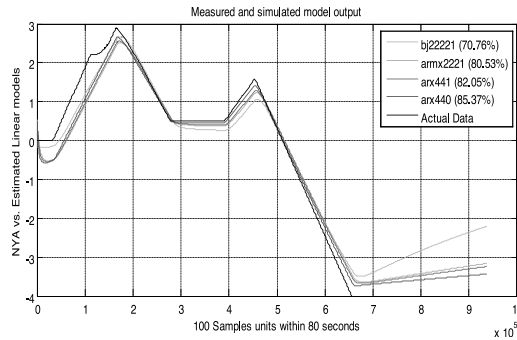


Fig. 13. Correlation between the measured data and identified models using different algorithms.

5.3. MPC Theory of Operation

The theory of Model Predictive Control is to utilize current and previous samples of the controlled variables measured at regular instances to produce current and future actions at a regularly spaced, discrete time instances. The interval separating successive samples is named the sampling period “ T_s ” (also called the control interval).

The MPC operation can be summarized in the following steps:

1. At each time step, compute the control actions (sequence) by solving an open-loop optimization problem for the prediction horizon.
2. Apply the first value of the computed control sequence.
3. Apply the Receding Horizon Control (RHC) step (Fig. 14).
4. At the next time step, get (measure/estimate) the system state and re-compute the control sequence.

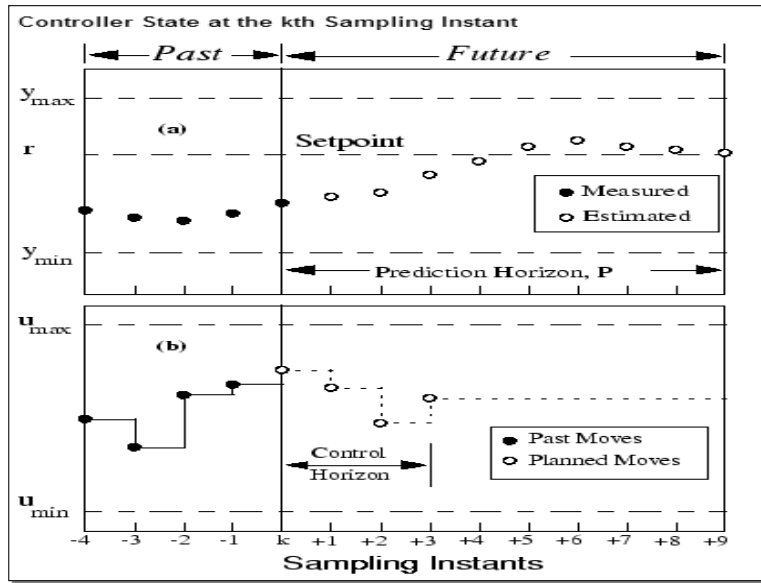
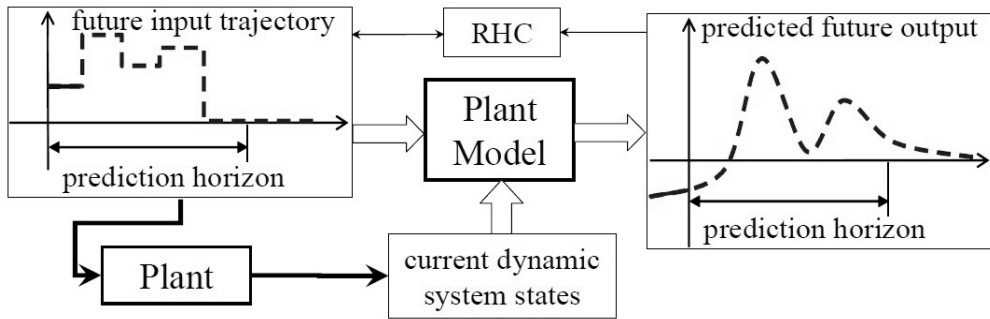


Fig. 14. MPC: Top: Block diagram showing the RHC step, Bottom: (a) measured plant outputs, (b) controller moves.

Fig. 14.a shows the latest measured output y_k , and previous measurements $y_{k-1}, y_{k-2} \dots$ etc., Fig. 14.b shows the controller's previous actions, $u_{k-4} \dots u_{k-1}$, as filled circles, where integer k represents the current instant.

To calculate its next action u_k , the controller operates in two phases:

1. **Estimation:** By knowing the current and past values of the controlled variables as well as any internal influencing variables that can affect the future trend, the controller can generate a stream of current and future (intelligent) actions. The controller uses built-in models to accomplish the estimation of the current and future moves.
2. **Optimization:** values of set-points, measured disturbances, and constraints are specified over a finite horizon of future sampling instants $k+1, k+2 \dots k+P$, where P (integer ≥ 1) is the prediction horizon. The controller computes M moves $u_k, u_{k+1} \dots u_{k+M-1}$, where M ($\geq 1, \leq P$) is the control horizon. In the example shown in Fig. 14, $P = 9$ and $M = 4$. The moves are the solution of a constrained quadratic optimization problem for the cost function given in (2) subject to the NYR as the constraint for the controller output.

$$J = (R_s - Y)^T (R_s - Y) + \Delta U^T \Gamma \Delta U \dots \dots \dots (2)$$

where the first term describes the minimization objective of the errors between the predicted outputs (Y) and the

set-point signals (R_s) and the second term consider the weight given to the size of the change of the control action ΔU when minimizing the objective function J is made, and \mathbf{F} is a diagonal matrix of size $(M \times M)$ in the form that $\mathbf{F} = r_w \mathbf{I}$ ($r_w \geq 0$), where r_w is used as a tuning parameter, which is assigned according to the desired performance.

MPC has many parameters to tune but from experimental trials, it has been noticed that the most effective parameter in our case is T_s , the sampling time, which almost has the effect of proportional gain of PID control, as the more T_s is being decreased, the more to reach steady state quickly but with the penalty of increasing overshoot. So, for an optimized response, good traction without overshoot as per the wind profile “Wind Direction 1”, the values of $T_s = 0.33$ sec, $P = 10$ and $M = 2$ are selected based on the excellent performance shown in Fig. 15, which tracks the wind direction correctly while respecting the NYR without any overshoot.

The developed MPC has been tested as well on the validation wind profiles “Wind Direction 2” and “Wind Direction 3” and has shown very good results as shown in Fig. 16 and Fig. 17.

6. PERFORMANCE COMPARISON

To evaluate the performance of the three control strategies studied in the paper, and to compare the effectiveness of each technique for best tracking the wind direction by the yaw actuation system, the Root Mean Square Error (RMSE) method is used. Three wind profiles are used for this comparison named “Wind Direction 1 (WD1)”, “Wind Direction 2 (WD2)”, and “Wind Direction 2 (WD2)”, respectively, with the results of the 80-seconds simulation span for each being shown in previous sections. The RMSE values are calculated and reported in Table 3.

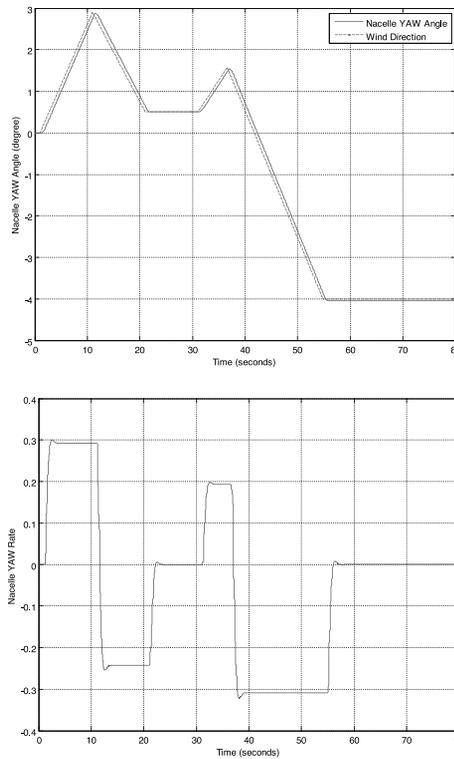


Fig. 15. MPC, Top: Nacelle Yaw Angle and “Wind Direction 1”, Bottom: Nacelle Yaw Rate.

Table 3. RMS of errors produced by each controller.

	WD1	WD2	WD3	Mean RMSE
PID	0.0967	0.1043	0.3836	0.1949
FLC	0.1518	0.1917	0.6521	0.3319
MPC	0.0966	0.1008	0.2016	0.1330

The results show that the MPC has the lowest RMSE, which indicates the best performance as expected. However, the PID controller shows comparable results to the MPC ones (although 47% more RMSE, but the bulk of it in the severe swing of wind direction scenarios like WD3) even though it is much simpler and easier to implement than the other two controllers.

The classical FLC shows significantly poor performance compared to the other two (150% more RMSE) especially in the WD3 test case where it shows extremely poor performance (223% more RMSE). The FLC has been carefully designed with extensive trials and incorporating the previous author’s experiences in this process (Farag *et al.*, 2016; Farag *et al.* 1996). However, by analyzing the results, it was clear that FLC is not able to react fast enough to the abrupt swing of wind directions due to the inherit inclusion of a derivative term in its design that delays/dampens the response (not the case in PI or MPC techniques). This result advocates the use of adaptive fuzzy logic techniques to cope with the unlimited scenarios of wind profiles, which is considered by the authors in future work.

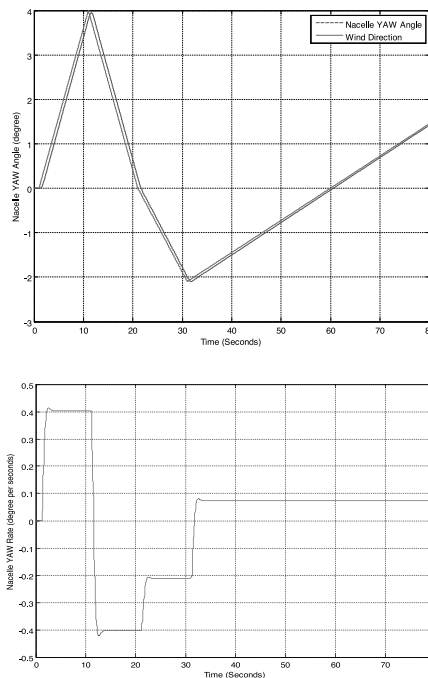


Fig. 16. MPC, Top: Nacelle Yaw Angle and “Wind Direction 2”, Bottom: Nacelle Yaw Rate.

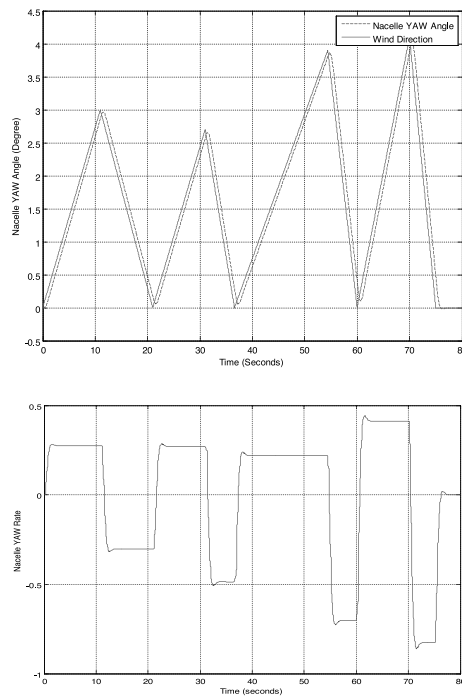


Fig. 17. MPC, Top: Nacelle Yaw Angle and “Wind Direction 3”, Bottom: Nacelle Yaw Rate.

The measured wind directions have significant uncertainties, which mandate discussing this matter within the scope of the three control techniques that have been studied in this paper. The superiority of the MPC in handling model uncertainties and external disturbances compared to the PID due to its inherent predictive and optimization phases is well known from the literature (Qin *et al.*, 2003). However, the FLC is well known as well for its outstanding performance in uncertain “fuzzy” environments (it is actually built with this purpose in mind) (Farg, 2005). Therefore, it is expected that both MPC and FLC will outperform the PID in this regard. However, still the MPC outperforms both other controllers in the main wind-direction tracking problem, which cements the conclusion that the MPC is the favorite control technique with the problem at hand.

7. CONCLUSION

For multi-MW wind turbines, nacelle yaw control is crucial for maximizing the energy harvest where misalignments between the nacelle and the wind direction cause considerable loss of generated power. This loss is proportional to Cos^3 of yaw angle error.

Accordingly, in this paper, three different and distinct yaw control strategies have been investigated. A carefully tuned PID controller has been designed and extensively simulated and the results of three wind profiles scenarios have been illustrated. Furthermore, a classical fuzzy logic controller with forty-nine rules and three scaling factors has been designed and validated as well using the same wind profiles scenarios. Moreover, a model predictive controller has been constructed from the collected input-output data of the simulated wind turbine under PID control. The MPC is validated using the same wind profiles scenarios. The mechanical constraints like nacelle yaw rate have been observed while designing the three controllers.

The evaluations and the comparative studies showed that the MPC has significantly outperformed the other two controllers. However, the PID controller showed acceptable performance and comparable to the MPC one. The FLC controller performance is far from satisfactory as it could not manage to track the abrupt swings in wind directions. Incorporating adaptive or self-organizing features in the fuzzy-logic controller design has to be researched in future work.

Finally, the presented study and the thorough analysis showed that the MPC controller is the best choice for the nacelle yaw control, regardless of the complexity of its design, but given the performance, it is justifiable. However, the carefully designed and fine-tuned PID controller is also applicable considering its simplicity, cost effectiveness, and performance. Additionally, the classical FLC performance is inferior to the PID one and cannot be used without augmenting adaptation of online tuning mechanism.

REFERENCES

- A. M. Hemeida, W. A. Farag & O. A. Mahgoub. 2011.** Modeling and Control of Direct Driven PMSG for Ultra Large Wind Turbines. *Intern Conf. of Nuclear and Renewable Energy Engineering (ICNREE 2011, 28-30 Nov., Venice, ITALY)*, pp 918-924, (WASET) 59 2011.
- A. Bemporad, M. Morari & N. L. Ricker. 2005.** Model Predictive Control Toolbox. pp. 11-18, March 2005.
- Ahmed M. Hemeida, Osama A. Mahgoub & Wael A. Farag. 2013.** Design of a Comprehensive 5MW Direct-Driven PMSG wind Turbine Emulator Using FAST nonlinear Wind Turbine Model. ISSN: 2325-7407, 2(4), Intern J. of Automation and Control Engineering, Nov. 2013.
- Chen FQ & Yang JM. 2009.** Fuzzy PID controller used in yaw system of wind turbine. IEEE 3rd International Conference on Power Electronics Systems and Applications, 2009. p. 1-4.
- Chenghui ZHU, Pengju LI, Jianping W & Xiaobing XU. 2011.** "Research on intelligent controller of wind-power yaw based on modulation of artificial neuroendocrine immunity system", *Procedia Eng* 2011; 15:903-7.
- Farret FA, Pfitscher LL & Bernardon DP. 2001.** Sensorless active yaw control for wind turbines. IEEE 27th Annual Conf. of the IEEE Industrial Electronics Society, 2001. p. 1370-75.
- Fadaeinedjad R, Moschopoulos G & Moallem M. 2009.** The impact of tower shadow, yaw error, and wind shears on power quality in a wind-diesel system. *IEEE Trans Energy Conversion* 2009; 24(1):102-11.
- Fernando G. Martins. 2005.** Tuning PID Controllers using the ITAE Criterion. *Int. J. Engng Ed.* Vol. 21, No. 5, pp. 867-873, 2005.
- Hamid Shariatpanah, Roohollah Fadaeinedjad & Masood Rashidinejad. 2013.** A New Model for PMSG-Based Wind Turbine with Yaw Control. *IEEE Trans. on Energy Conversion*, Vol. 28, No. 4, Dec. 2013.
- H. M. Hassan, W. A. Farag, Abdel Latif ElShafei & M. S. Saad. 2011.** Designing Pitch Controller for Large Wind Turbines via LMI Techniques", *Energy Procedia*, Elsevier, pp 808-818, vol. 12, 2011.
- H. M. Hassan, W. A. Farag, M. S. Saad & A. L. Elshafei. 2012.** Adaptive Look-Ahead Feed-forward Wind Turbine Pitch Control using LIDAR Technology. *Intern Conf. on Sustainable Systems and Technologies*, (WASET) 65 2012, Amsterdam, May 13, 2012, pp 675-681.
- H. M. Hassan, W. A. Farag, M. S. Saad & A. L. Elshafei. 2012.** Robust Dynamic Output Feedback Pitch Control for Flexible Wind Turbines. *IEEE EnergyTech*, May 29, Cleveland, Ohio, USA.
- H. M. Hassan, W. A. Farag, A. L. ElShafei & M. S. Saad. 2012.** A Robust LMI-Based Pitch Controller for Large Wind Turbines. *Renewable Energy*, v.44, 2012 August, p.63(9) (ISSN: 0960-1481), Elsevier.
- H. M. Hassan, W. A. Farag, Abdel Latif ElShafei & M. S. Saad. 2011.** Design of Multi-Objective Robust Pitch Control for Large Wind Turbines. *World Congress on Sustainable Technologies*, pp 95, Nov. 7-10, 2011, London, UK.
- Kusiak A, Zheng H & Song Z. 2010.** Power optimization of wind turbines with data mining and evolutionary computation. *Renewable Energy* 2010; 35(3):695-702.
- L. Wenzhou, C. Changqing & Z. Zhuo. 2011.** Design of a large scale wind turbine generator set yaw system. *IEEE Inter. Conf. on Computer Science and Edu.*, Singapore, August 2011.
- L. Wang. 2009.** Model Predictive Control System Design and Implementation Using MATLAB. ECE Dept., RMIT University, 2009.
- Lee K, Im J, Choy I, Cho W & Back J. 2011.** MPPT and Yawing control of a new horizontal-axis wind turbine with two parallel-connected generators. *IEEE 8th International Conference on Power Electronics-ECCE Asia*, 2011. p. 2618-24.

- M-G Kim & P. H. Dalhof. 2014.** Yaw Systems for wind turbines - Overview of concepts, current challenges, and design methods. *Journal of Physics: Conference Series* 524 (2014) 012086.
- M. Yesilbudak, S. Sagiroglu & I. Colak. 2015.** A novel intelligent approach for yaw position forecasting in wind energy systems. *Elec. Power and Energy Sys.* 69 (2015) 406–413, Elsevier.
- M. S. S. Santoso. 2011.** Dynamic Models for Wind Turbines and Wind Power Plants. NREL national laboratory of the U.S. Department of Energy, pp. 15-17, May 2011.
- Rijanto E, Muqorobin A & Nugraha AS. 2011.** Design of a yaw positioning control system for 100 kW horizontal axis wind turbines based on on/off control with dead band and hysteresis. *Int J Appl Eng Res* 2011; 6(19):2327–40.
- S. Miller. 2013.** Wind Turbine Model. *Mathwork. Inc*, March 2013.
- S. Miller. 2009.** <https://www.mathworks.com/videos/determining-mechanical-loads-for-wind-turbines-81627.html>, Video Webinar, *Mathwork. Inc*.
- S. Miller. 2017.** <https://www.mathworks.com/matlabcentral/fileexchange/25752-wind-turbine-model>.
- S. Joe Qin & Thomas A. Badgwell. 2003.** A survey of industrial model predictive control technology. *Control Engineering Practice*, Volume 11, Issue 7, July 2003, Pages 733-764.
- Wael Farag, Hanan El-Hosary, Khaled El-Metwally & Ahmed Kamel. 2016.** Design and implementation of a variable-structure adaptive fuzzy-logic yaw controller for large wind turbines. *Journal of Intelligent & Fuzzy Systems* 30 (2016) 2773–2785, IOS Press.
- Wael Farag, Hanan El-Hosary, Ahmed Kamel & Khaled El-Metwally. 2017.** A Comparative Study and Analysis of Different Yaw Control Strategies for Large Wind Turbines. *Intl Conf. on Advanced Control Circuits Systems (ACCS)*. pp 132-139, Nov. 5, 2017, Alexandria, Egypt.
- Wael A. Farag, V.H. Quintana & G. Lambert-Torres. 1996.** Neural Network-Based Self-Organizing Fuzzy Logic Automatic Voltage Regulator for a Synchronous Generator. 28th Annual North American Power Symposium (NAPS'96), pp. 289-296, Nov. 10 -12, 1996, MIT, Cambridge, Massachusetts, USA.
- W. A. Farag, H. M. Hassan, M. S. Saad & Abdel Latif ElShafei. 2017.** A LiDAR-based Pitch Control Strategy for Ultra Large Wind Turbines. *19th International Middle East Power Systems Conference (MEPCON)*, pp 451-458, Dec. 19, 2017, Cairo, Egypt.
- WA Farag. 2005.** Extraction of Fuzzy-Control Rules from the Input-Output Properties of a Controlled Plant. 1st IFAC Intern workshop on Advanced Control Circuits and Systems (IFAC ACCS'05), Cairo, Egypt, March 06-10, 2005.

Submitted: 21/03/2017

Accepted: 04/07/2018

تحليل تقنيات التحكم المختلفة فى الإنحراف الأفقى لتوربينات الرياح الكبيرة

*وائل فرج، منال الحصري، أحمد كامل وخالد المتولي
 *قسم الهندسة الكهربية، جامعة الشرق الأوسط الأمريكية، الكويت
 قسم القوى والآلات الكهربية، جامعة القاهرة، مصر

الخلاصة

فى هذا البحث، نقدم ثلاثة تقنيات مختلفة للتحكم فى الإنحراف الأفقى لجسم توربينه الرياح الكبيرة. التقنيات المقدمة تستخدم خوارزميات متميزة لتحسين التقاط طاقة الرياح وسوف يتم دراستها بالتفصيل. أول تقنية هى خوارزم المتحكم التناسبي-التكاملي-التفاضلي (PID) الذى تم تصميمه وتهيئته بعناية. والتقنية الثانية هى باستخدام المنطق اللغوى المشوش (linguistic fuzzy logic) والذى تم تصميمه بطريقة مرنة وبديهية. التقنية الثالثة تستخدم متحكم ذو نموذج تنبؤى ووظيفة تكيفية. الهدف الرئيسى من كل تقنيات التحكم المقدمة هو التتبع الفعال لحركة واتجاه الرياح من خلال الحركة الأفقية لجسم التوربينه؛ وبالتالي تحسين التقاط الطاقة. وسيتم إجراء دراسة مقارنة وتحليل شامل بين أداء تقنيات التحكم الثلاثة من خلال محاكاة واسعة النطاق باستخدام (MATLAB /SIMULINK).